Int. J. Electrochem. Sci., 11 **(2016)** 7198 – 7215, doi: 10.20964/2016.08.67

International Journal of ELECTROCHEMICAL SCIENCE
www.electrochemsci.org

Role of Some Plating Parameters in the Properties of Ni-P/Al_2O_3 Nanocomposite Coatings on Mg alloy

Fakiha El-Taib Heakal[1,*], *Maanoum A. Maanoum*[2]

[1] Chemistry Department, Faculty of Science, Cairo University.Giza 12613, Egypt.
[2] Central Metallurgical Research and Development Institute (CMRDI), Cairo, Egypt.
[*]E-mail: fakihaheakal@yahoo.com, feltaibheakal@gmail.com

Received: 3 April 2016 / *Accepted:* 17 June 2016 / *Published:* 7 July 2016

Electroless Ni-P/Al_2O_3 nanocomposite coatings on AZ91D magnesium alloy have been deposited by incorporating nanoalumina particles into Ni-P alloy matrix to stimulate the wear and corrosion resistance of the substrate. NanoAl_2O_3 particles were uniformly suspended in the bath for 1 h using magnetic stirring, and the Al_2O_3 content in the composite was determined gravimetrically. The effect of nanoparticle concentration in the plating bath on each of nanoAl_2O_3 in the deposit, its deposition rate, and its micro-hardness and wear resistance was thoroughly studied. The influence of SLS surfactant as a wetting agent on the porosity of the deposit and on its content from the nanoparticles was explored. Coat micro-hardness as well as phase transition were also examined in relation to temperature of the heat treatment process. Furthermore, the impact of bath temperature on the deposition rate and on the amount of incorporated nanoparticles in the deposit was discussed. The role of other plating parameters such as stirring speed and nickel sulfate concentration of the plating bath solution in determining the amount of nanoparticles embedded in the Ni-P matrix were assessed and rationalized. Electrochemical polarization curves were measured to evaluate the corrosion performance of AZ91D alloy samples coated with different prepared nanocomposite deposits. In all cases, the obtained as-plated or heat treated Ni-P/Al_2O_3 nanocomposite coating can perfectly act as a potential physical barrier to protect AZ91D substrate from corrosion in the aggressive chloride environment.

Keywords: EN nanocomposite; magnesium alloy; XRD; polarization curves; corrosion protection.

1. INTRODUCTION

Electroless Ni-P (EN) plating is an attractive engineering coating primarily used to prevent wear and corrosion, as well as an alternative for hard chromium deposit, which is very harmful to the environment and human health as it contains highly toxic carcinogens [1]. EN deposition is an autocatalytical reduction process of Ni ion from an aqueous solution containing sodium hypophosphite

as a metal-reducing agent without the use of electrical energy [2]. The as-deposited EN is a metastable supersaturated alloy with phosphorus and thus it differs significantly from electroplated nickel, where the coating properties can be tailored by optimizing the alloy composition. The variation in phosphorus content of EN is typically between 5 to 12 wt.% [3]. To improve EN coatings properties to suit several technical applications, EN composite deposits were developed, which involve the dispersion of tiny solid particles in the Ni-P matrix. This has been attempt to benefit the advantages of their inherent uniformity, hardenability, their unusual combination of wear and corrosion resistance properties [4].

For the meantime, magnesium alloys have continued increasing applications in wide-spread technical sectors and industries, owing to their high strength-to-weight ratios, good castability, high ductility, thermal and electrical conductivities, as well as desirable mechanical properties [5-8]. However, magnesium alloys are highly active materials, having poor atmospheric corrosion and wear resistance, which restrict their extensive utilizations [9,10]. For that, various surface treatments have been applied to magnesium materials to improve their corrosion resistance, as for example anodization [11,12], deposition of chemical conversion layers [13,14], treatment based on the sol-gel applications [15]. On the other hand, electroless Ni-P plating is one of the most effective surface treatment techniques to overcome the defects of magnesium alloys as it can offer excellent properties of hardness, wear resistance and corrosion resistance by forming a uniform deposit on the magnesium alloy substrate [5,16-20]. In this direction, the past decade has witnessed increased attention towered incorporation of nanometer size particles in the deposits, as they are able to improve the tribological properties of the coatings through modification of the growing crystalline nickel film [21-23] and creation of dispersion hardening effects at low incorporation level [21,24]. Nevertheless, the mechanism of nanoparticle incorporation in EN matrix has received little attention. Therefore, the main intent of the present work is to fabricate and test various electroless Ni-P/Al_2O_3 nanocomposites on AZ91D alloy subatrate in order to assess the role of some important plating parameters in the properties of the obtained coatings. The studied properties include the amount of Al_2O_3 nanoparticles in the deposit, its deposition rate, micro-hardness, wear and corrosion resistance, as well as its porosity and crystallinity. The experimental parameters involve each of the following: concentration of Al_2O_3 nanoparticles in the plating bath, wetting agent, post-heat treatment temperature of the deposit, temperature of the plating bath, and the agitation speed of its solution, as well as concentration of its nickel ions.

2. EXPERIMENTAL

The AZ91D magnesium alloy was supplied from National Company for Metals, (Helwan, Egypt) as rolled sheets of thickness 3.0 mm and chemical composition in wt.% of: 9.0 Al, 0.68 Zn, 0.18 Mn, 0.001 Ni, 0.001 Cu, < 0.001 Fe, < 0.001 Si, and balance Mg. Rectangular samples with size 15 mm x 10 mm, were cut, prepared and coated using the electroless plating technique according to the following steps. (i) The samples were mechanically abraded with emery paper up to 1200 grit finish, then cleaned with acetone in an ultrasonic cleaning bath. (ii) Alkaline cleaning in (25 g/L Na_2CO_3 + 15 g/L NaOH) solution for 5 min at 65 ^oC. (iii) Acid pickling in (120 g/L CrO_3 + 100 ml/L HNO_3)

solution for 5 s at room temperature, followed by fluoride activation in (100 g/L NH_4HF_2 + 200 ml/L H_3PO_4) solution for 60 s at 65 ^oC. (iv) Alkaline activation in (40 g/L $Na_4P_2O_7$ + 70 g/L $Na_2B_4O_7.10H_2O$ + 20 g/L NaF) solution for 10 min at room temperature. (v) Zincating treatment in (30 g/L $ZnSO_4.6H_2O$ + 120 g/L $Na_4P_2O_7$ + 5 g/L NaF) solution for 5 min at room temperature. (vi) Electroless nickel plating at 85 ^oC from acidic bath (pH 4.5) containing in g/L: 30 $NiSO_4.6H_2O$ + 20 $NaH_2PO_2.2H_2O$ + 15 trisodium citrate ($Na_3C_6H_5O_7.2H_2O$) + 10 CH_3COONa + 0.002 thiourea + 0.002 sodium lauryl sulfate. Before electroless plating, the nanocomposite coatings were prepared by adding to the electroless bath different concentrations (over the domain 5-20 g/L) from Al_2O_3 nanoparticles of size 100 nm. The nanoparticles were kept uniformly suspended in the bath solution using magnetic stirring for 1 h to insure sufficiently dispersed particle in the final nickel coating. The nanoAl_2O_3 content in the composite was determined gravimetrically using four decimal microbalance. The deposition rate was determined from the weight gain ($\Delta w = w_2 - w_1$), where w_1 and w_2 are respectively, the weight of AZ91D sample before and after EN composite coating. All solutions used were freshly prepared from analytical grade reagents and deionized water. Water rinse were applied after each step. Due to the high reactivity of magnesium alloys, the zincating pre-treatment has been used to remove the residual oxides and hydroxides and to produce a thin layer of zinc to prevent re-oxidation of the substrate surface as has been previously reported [5,25]. Some coated samples were further heat treated at various temperatures of 250^o, 300^o, 350^o and 400 ^oC in an air muffle furnace whose temperature can be controlled within 1 ^oC. The nanocomposite coated samples were maintained for 1 h at the setting temperature, then gradually air cooled to the room temperature. The micro- hardness, wear and corrosion resistances of the samples have been also determined. The micro-hardness of nanocomposite coatings was measured using a diamond pyramid indentor 100 g under load for 1 s. More than 15 indentations were made on each sample on the cross sections. Only the readings corresponding to full indentation away from the AZ91D substrate were taken into consideration. For the effect of wetting agent, sodium lauryl sulfate (SLS) surfactant was used within the concentration range 0-25 mg/L in the acidic EN bath solution. The coating porosity before and after heat treatment was evaluated by the combination of corrodkote and filter paper test. Each coated sample was immersed for 5 min in the corrodkote solution (5 ml HCl + 6 g NaCl in 100 ml water). Due to corrosion, the substrate ions released through the opening holes gave a color reaction after 3 min immersion in eriothrome black T indicator solution (0.5 g L^{-1}). Then, the sample was immediately taken onto a filter paper, where the number of color spots (n) was counted and the porosity was given as n/s, s being the coating surface. The wear resistance for nanocomposite coatings prepared from EN baths containing different concentrations of nanoAl_2O_3 particles was performed on tribometer machine. The effect of thermal treatment on the crystalline structure of the deposits was studied using a Siemens D 5000/Kristalloflex diffractometer in the $\Theta/2\Theta$ modus with CoKα radiation (40 kV, 40 nA). An adjustable sample holder was used to position the sample surface in the incidence plane of X-rays. Peaks were identified using a standard data base.

The surface morphology of the nanocomposite coating was determined using scanning electron microscop (SEM), JEOL 5410 with an accelerating voltage of 30 kV. The corrosion behavior of the samples in 3.5% NaCl solution at room temperature was also investigated using potentiodynamic polarization technique. Measurements were performed in a conventional three electrode glass cell

furnished with a saturated calomel reference electrode (SCE). The coated sample with an exposed surface of 1 cm^2 and a large platinum sheet were utilized as working and counter electrodes, respectively. The DC polarization curves were traced at a scan rate of 2 mV/s within the applied potential range from -2.5 V to 2.0 V (vs. SCE) using Wenking LB 94 Laboratory Potentiostat [P_1]. Prior polarization, the open circuit potential (OCP) of AZ91D sample in 3.5% NaCl solution was measured till the potential became constant with time for a period of 30 min.

3. RESULTS AND DISCUSSION

3.1. Effect of nanoAl_2O_3 concentration in the bath

3.1.1. Nano Al_2O_3 content in the deposit

Electroless Ni-P/Al_2O_3 nanocomposite coatings were fabricated by dispersing inert Al_2O_3 nanoparticles in the plating solution and co-deposited some of these distributed particles within the Ni-P metallic matrix. The Al_2O_3 nanoparticles with size of ~100 nm were kept uniformly suspended in the bath for 1 h using magnetic stirring. The wt.% of Al_2O_3 nanoparticles incorporated in the Ni-P/nanocomposite coatings, as determined gravimetrically, was found to be a function of the Al_2O_3 nanoparticle concentration in the plating bath (in g/L).

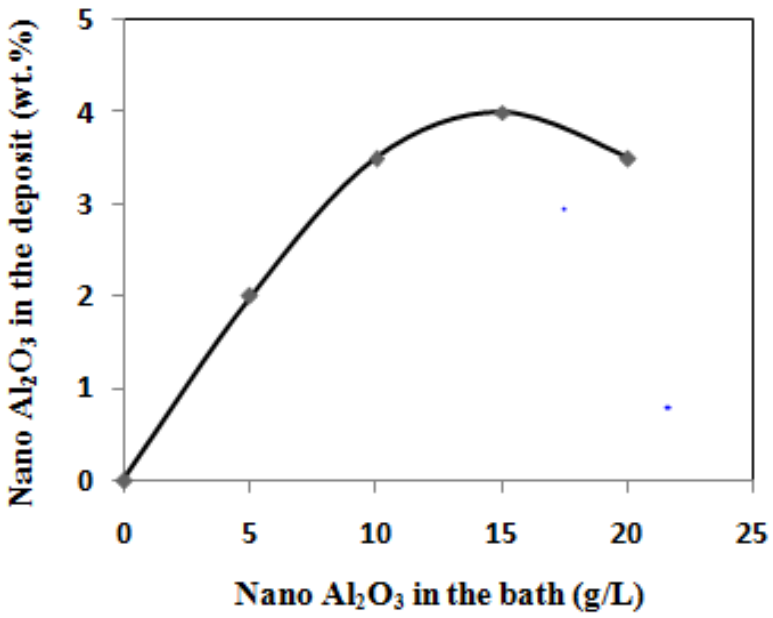

Figure 1. Effect of nanoAl_2O_3 concentration in the electroless plating bath solution on the nanoAl_2O_3 content in the deposit.

The obtained results shown in Fig. 1 demonstrates a fast increase in the concentration of nanoAl_2O_3 particles in the deposit up to a maximum value of 4 wt.% with increasing the amount of homogeneously distributed nanoalumina in the plating solution up to a concentration of 15 g/L. After then, the incorporated Al_2O_3 nanoparticle in the coat decreases as its concentration in the EN bath is

further increased more than 15 g/L. This decrease may be a result of possible particles agglomeration in the bath solution, as the degree of this process is expected to increase with raising the amount of dispersed phase in the electrolyte [4,26]. It follows that a decreasing trend is obtained after the threshold concentration (15 g/L).

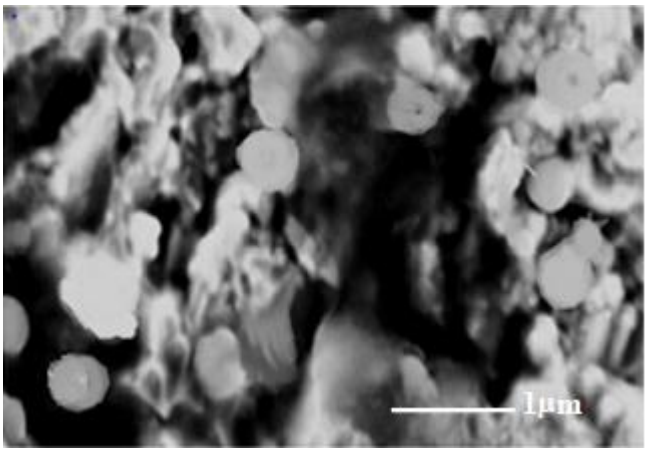

Figure 2. SEM image of nanoAl_2O_3 particles in the Ni–P/Al_2O_3 nanocomposite coating.

As can be seen from the microstructure image of Al_2O_3 nanocomposite coating presented in Fig. 2, the morphology of Al_2O_3 nanoparticles has nearly spherical shape with diameter in the range of ~100 nm. The nanoparticles are located at different elevations over amorphous grain structure of electroless Ni-P matrix with random distribution and interstices among them.

3.1.2. Deposition rate

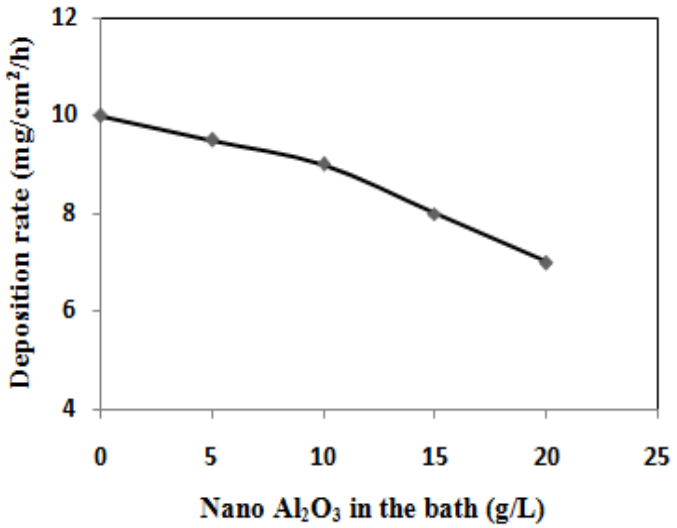

Figure 3. Effect of nanoAl_2O_3 concentration in the electroless plating bath solution on the deposition rate of Ni-P/Al_2O_3 nanocomposite coatings.

The deposition rate (in mg/cm^2/h) of Ni-P/Al_2O_3 nanocomposite on AZ91D substrate is also measured as a function of the nanoalumina concentration in the plating solution (in g/L). Fig. 3 reveals that upon increasing the load of nanoalumina particles in the plating bath over the range 0-20 g/L, the deposition rate of the nanocomposite coating decreases. This may be ascribed to an increase in the number of physically adsorbed nanoalumina particles onto the substrate surface, leading to decreasing its available active sites for the deposition process, with a subsequent decrease in the overall deposition rate [27].

3.1.3. Micro-hardness and wear resistance

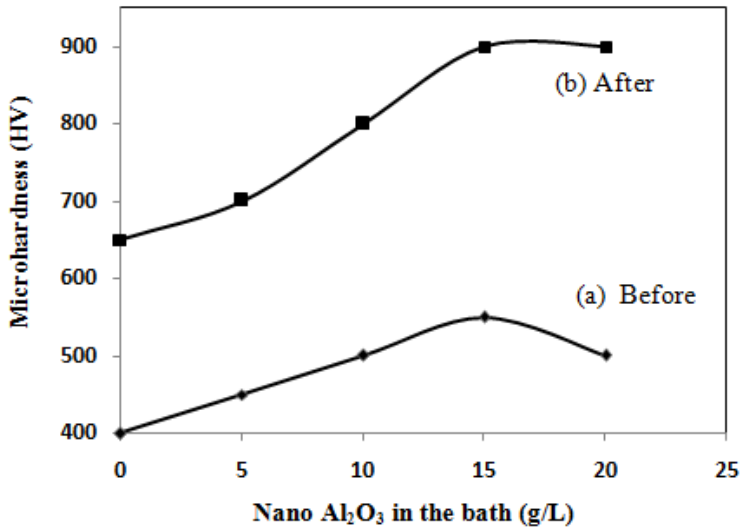

Figure 4. Effect nanoAl_2O_3 concentration in the electroless plating bath solution on micro-hardness of Ni-P/Al_2O_3 nanocomposite coatings (a) before and (b) after heat treatment at 350 ^oC for 1 h.

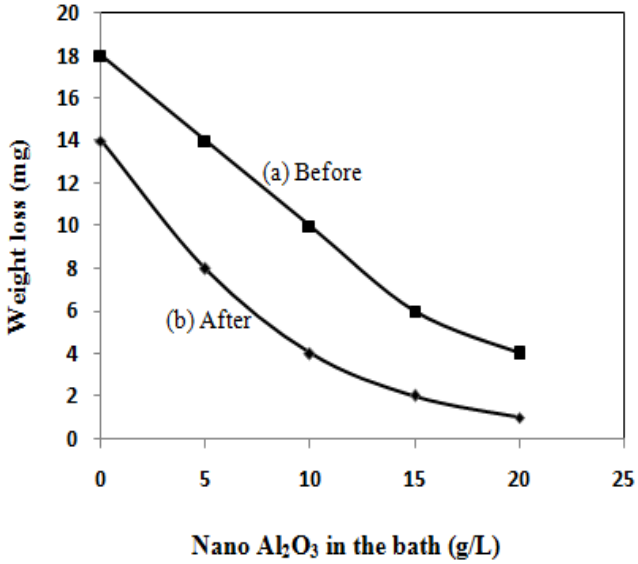

Figure 5. Effect of nanoAl_2O_3 concentration in the electroless plating bath solution on wear resistance of Ni-P/Al_2O_3 nanocomposite coatings (a) before and (b) after heat treatment at 350 ^oC for 1 h.

Fig. 4 shows the effect of nanoAl_2O_3 particles concentration in the bath on the micro-hardness of electroless Ni-P/Al_2O_3 nanocomposite coatings before and after heat treatment. The hardness of the composite coating increases with increasing nanoAl_2O_3 particle concentration in the plating bath, and increases also as a result of heat treatment at 350 ^oC for 1 h. Formation of Ni_3P during heat treatment process is believed to be responsible for introducing hardness effect that improves the performance of electroless Ni-P/Al_2O_3 nanocomposite coatings.

On the other hand, Fig. 5 demonstrates variation of the wear rate in terms of weight loss in electroless Ni-P/Al_2O_3 nanocomposite coating, as a function of alumina nanoparticle concentration in the bath. The results indicate a significant decrease in the weight loss with increasing loading of nanoalumina in the bath as well as after heat treatment of the coated sample at 350 ^oC for 1 h. It follows that, AZ91D surface with superior wear resistance performance can thus be achieved after heat treatment of electroless Ni-P/Al_2O_3 nanocomposite coating prepared from a bath containing the highest possible nanoAl_2O_3 particles concentration, being equal to 20 g/L in the present work. Also, one can conclude that for as-plated or heat treated samples hard evenly dispersed nano-particles can greatly enhance the wear resistance of the composite coatings as compared with bare electroless Ni-P coatings having no alumina nano-sized particles as reinforcement for composite coatings [4].

3.2. Effect of wetting agent

3.2.1. NanoAl_2O_3 content in the deposit

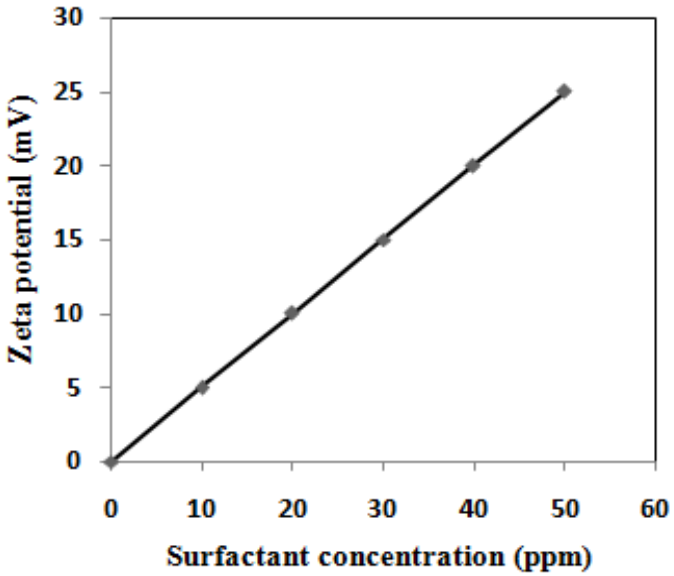

Figure 6. Effect of sodium lauryl sulfate (SLS) surfactant concentration on the Zeta potential of nano Al_2O_3 particles.

The Al_2O_3 nanoparticles are difficult to stay dispersed in the EN solution for a prolonged time unless treated with a special surface active agent or wetting agent. Modifying the electroless nickel plating bath using special additives, such as surfactants, plays a major role in deciding incorporation of

the second phase particles in the binary Ni-P matrix. A better understanding of the surfactant adsorption on the substrate is essential to achieve higher level of incorporation. For the present work, the wetting agent used to disperse Al_2O_3 nanoparticles in the plating solution is sodium lauryl sulfate (SLS) as an anion surfactant ($CH_3(CH_2)_{11}OSO_3^-\ Na^+$) [28], together with the optimal concentration of Al_2O_3 nanoparticles in solution, namely the critical concentration of 15 g/L.

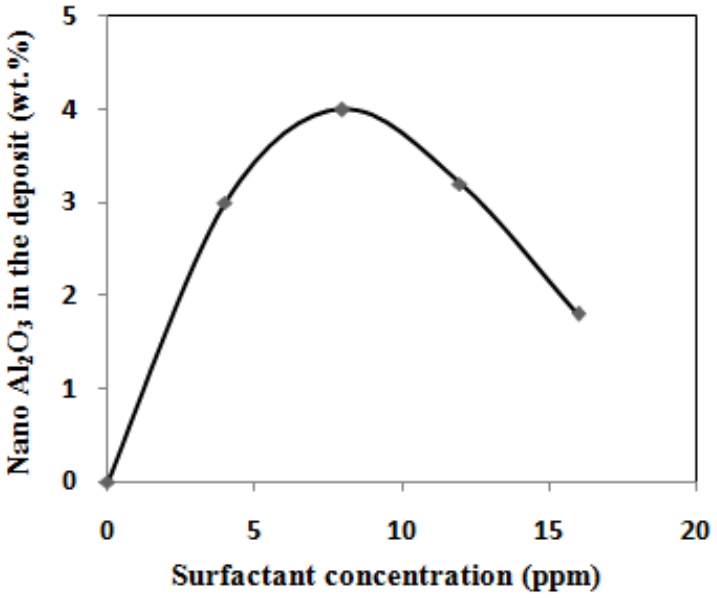

Figure 7. Effect of surfactant concentration (SLS) in the electroless plating bath on the nano Al_2O_3 content in the deposit.

Fig. 6 indicates that the Zeta potential of Al_2O_3 nanoparticles in the plating solution containing SLS, increases linearly with increasing surfactant concentration. Such behavior implies continuous increase in the stability of suspended Al_2O_3 nanoparticles in solution, induced by the saturated adsorption of surfactant molecules on the particle surfaces. It is known that suspension stability is directly related to the increase in the wettability of its suspended particles via adsorbed surfactant anions on their surfaces. This will then prevent agglomeration of the particles and preclude their electrostatic attraction [26].

Fig. 7 shows clearly that the amount of Al_2O_3 nanoparticles increases in the electroless Ni-P deposit with increasing surfactant concentration rapidly at first, then gradually slow down till reaching an optimum concentration of 8 ppm. Afterward, further increase in surfactant concentration produces an adverse effect on the incorporated Al_2O_3 nanoparticles in the electroless Ni-P matrix. Adsorbed surfactant molecules onto the nanoalumina are embedded in the deposit together with the nanoparticles. Nevertheless, a relatively small amount of adsorbed surfactant will hardly affect the deposit properties. However, free surfactant molecules which are not adsorbed on the Al_2O_3 nanoparticles are co-deposited with the metal, resulting in stressed and brittle deposits. Celis et al. [29,30] have proposed a model describing the role of surfactant molecules during the deposition of Cu-Al_2O_3 composite coatings. Similar model can be postulated for the formation of the present Ni-

P/Al_2O_3 nanocomposite deposits on AZ91D substrate.

3.2.2. Porosity of the deposit

It is generally accepted that the autocatalytic EN deposition is initiated by catalytic dehydrogenation of the reducing agent with the release of hydride ions, in which then the hydride ions supply electrons for the reduction of nickel ion, accompanied the H_2 gas produced [31]. Fig. 8 reveals that upon increasing surfactant concentration in the EN/Al_2O_3 nanocomposite plating bath over the domain 0-25 ppm SLS, the number of pores/cm^2 decreases for both as-plated and heat-treated coatings [32].

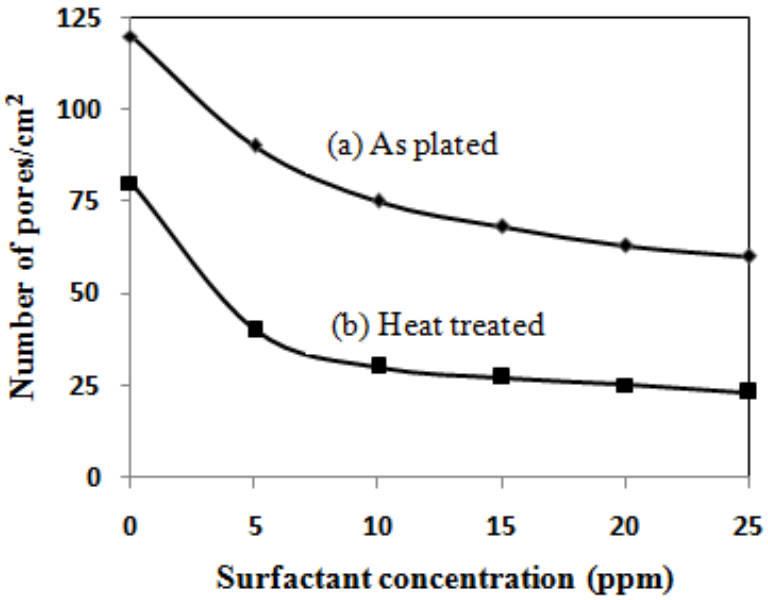

Figure 8. Effect of wetting agent on the porosity of as-plated and heat treated electroless Ni-P/nano Al_2O_3 composite coatings.

This indicates that the wetting agent (SLS) can promote releasing hydrogen bubbles from the substrate surface. If these bubbles are allowed to adhere on the substrate, they would prevent the plating process at the sites of bubbles resulting in increasing the porosity of the composite deposits [31]. The present results demonstrate that addition of wetting agent at very low concentration can reduce the surface tension of electroless nickel solution in the plating bath, thereby preventing attachment of hydrogen bubbles to the substrate surface. For example, on comparing the porosity of the prepared deposit from SLS-free bath solution with that prepared from plating solution containing 25 ppm SLS, the number of pores decreases from 120 pores/cm^2 to almost half its value (~ 60 pores/cm^2), respectively. Additionally, if this latter sample was heat treated at 350 ^oC for 1 h its porosity is further decreased to only 25 pores/cm^2. The reason for that is because the grains size for the heat treated coat are always larger than those for the as-plated Ni-P/Al_2O_3 nanocomposite coatings, despite the added amount from the surfactant. Generally, the morphology of the deposits are all similar

but their grain sizes become bigger after the process of heat treatment. Recently, it has been reported that globules of Ni-P/Al_2O_3 composite coating become compact after heat treatment at 400 ^oC, which results in reducing its porosity [32].

3.3. Effect of heat treatment temperature

3.3.1. Coat micro-hardness

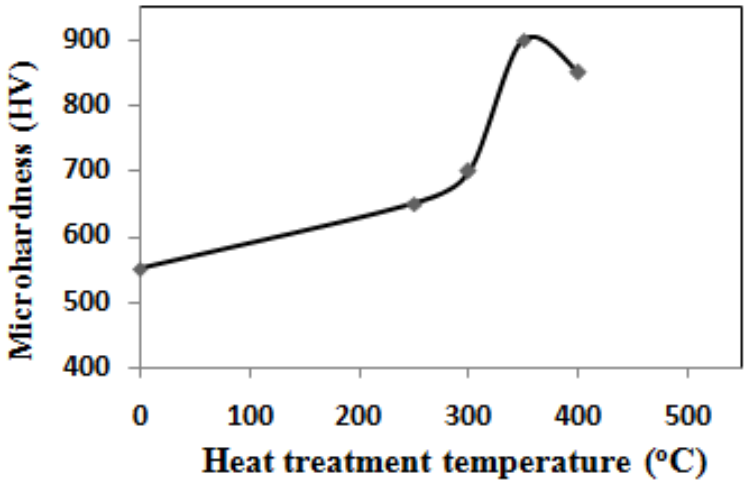

Figure 9. Effect of heat treatment temperature on micro-hardness of electroless Ni-P/nanoAl_2O_3 composite coatings.

Fig. 9 shows the micro-hardness variation of Ni–P/Al_2O_3 nanocomposite coatings with the temperature at which heat treatment process was conducted. As can be seen, the as-plated electroless Ni–P/Al_2O_3 nanocomposite coating has micro-hardness of 550 HV. Generally, the micro-hardness increases for the heat treated samples, due to the effect of dispersion strengthening generated by Al_2O_3 nanoparticles during coat annealing, as well as due to formation and fine dispersion of the harden coherent intermetallic Ni_3P phase [33]. The heat-treated nanocomposite coating annealed at 250 ^oC for 1 h achieves a micro-hardness of 650 HV, which increases till a maximum value of 900 HV upon raising the annealing temperature to 350 ^oC. However, further increase in the temperature of heat treatment up to 400 ^oC leads to a slight decrease in the value of its micro-hardness. The decrease in hardness when these coatings are annealed at and beyond 400 ^oC can be traced to the over aging of the composites which causes grain coarsening for both Ni-P matrix and Ni_3P phase [34].

3.3.2. Amorphous-to-crystalline phase transformation

It has been reported that for composite and nanocomposite coatings, the particles are attached physically to the Ni-P matrix [4,26]. Thereby, heat treatment process for these coatings is necessary in

order to promote phase transformation, which would influence the adherence and some properties of the deposited layers [35].

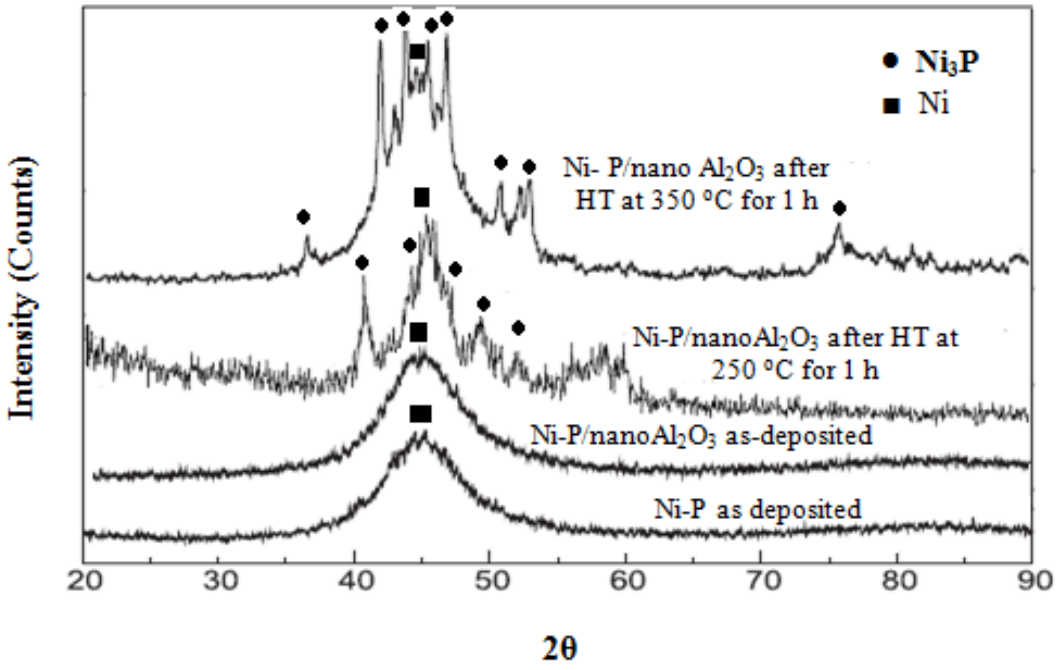

Figure 10. XRD patterns of electroless Ni-P and Ni-P/Al_2O_3 nanocomposite coatings as-deposit and after heat treatment for 1 hour at 250 °C and 350 °C.

Fig. 10 presents the XRD patterns of Ni–P/nanoAl_2O_3 composite coatings before and after heat treatment at 250 ^oC and 350 ^oC for 1 h. The following points can be withdrawn from this figure. (i) The existence of Al_2O_3 nanoparticles does not change the metallic matrix structure, since EN deposit and its nanocomposite deposit are both amorphous. (ii) The inclusion of Al_2O_3 as nanometer-sized particles in the Ni–P alloy coating facilitates its crystallization process and lowers the crystallization temperature. (iii) Intermetallic nickel phosphide (Ni_3P) phase precipitates in the composite coating after heat treatment at 250 ^oC for 1 h, and its amount becomes higher upon raising the temperature of the heat treatment process to 350 ^oC.

3.4. Effect of bath temperature

3.4.1. Deposition rate

The deposition rate of electroless Ni-P/Al_2O_3 nanocomposite coating as a function of bath temperature is given in Fig. 11. The experimental data indicate that over the range 60-90 ^oC the deposition rate increases with increasing bath temperature, so that the co-deposition of Al_2O_3 nanoparticles in the EN metallic matrix increases. However, above this range of temperature electroless nickel bath becomes unstable and the plating solution starts to decompose.

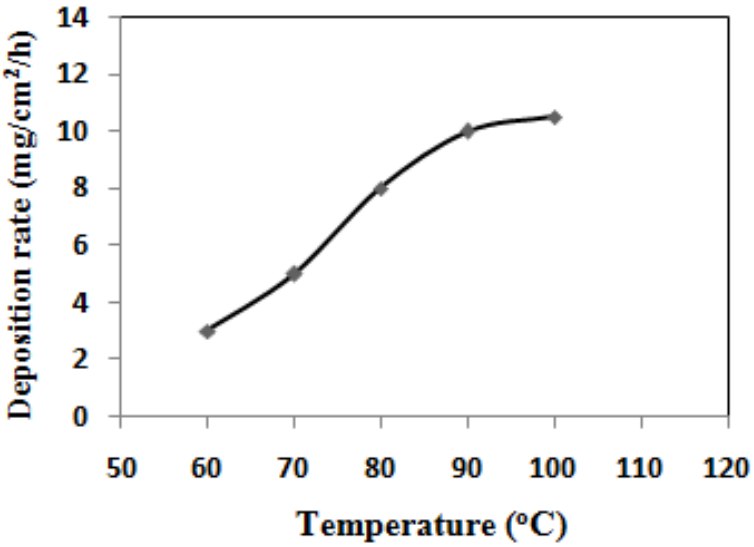

Figure 11. Effect of electroless nickel bath temperature on the deposition rate of Ni-P/Al_2O_3 nano-composite coatings.

3.4.2. Nano Al_2O_3 in the deposit

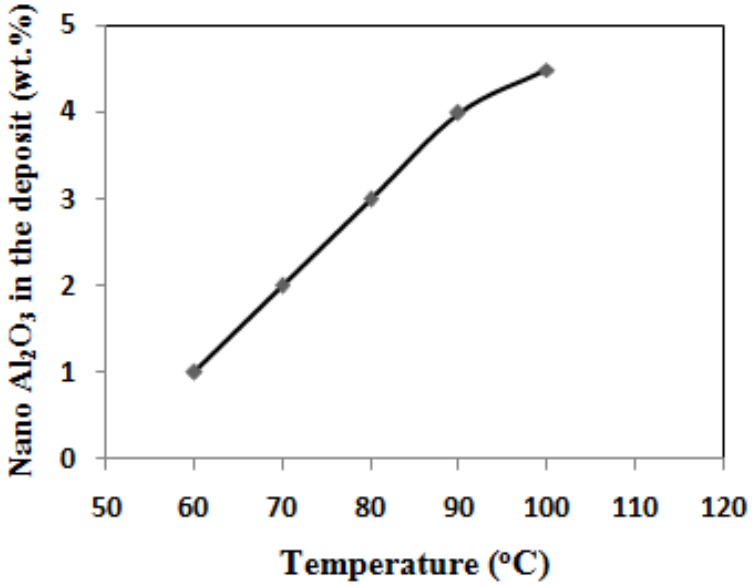

Figure 12. Effect of electroless nickel bath temperature on the nanoAl_2O_3 content in the deposit.

Experimental results shown in Fig. 12 clearly indicate a steep linear increase in the weight percentage of embedded Al_2O_3 nanoparticles in the Ni-P coatings with raising bath temperature up to 90 ^{o}C. Above this temperature the bath becomes unstable, thus a small effect is observed. It is well established that temperature is among the several factors controlling the physical stability in suspensions.

Increasing temperature of a nanofluid increases the physical stability in suspension due to superior thermal conductivity and diffusivity of its nanoparticles [36]. Accordingly, a big reduction in

the force of resistance to movement of alumina nanoparticles dispersed inside the electroless nickel bath solution, which enhances their dispersability and increases the amount of their incorporation in the composite coatings.

3.5. Effect of bath agitation

Agitation of the plating solution is also a key factor in determining alumina nanoparticles incorporation. This is because the nanoparticles are in need to reach their destination on the substrate in order to be embedded in the Ni-P matrix, thereby must have a mean to be transported from bulk of solution to the metallic surface.

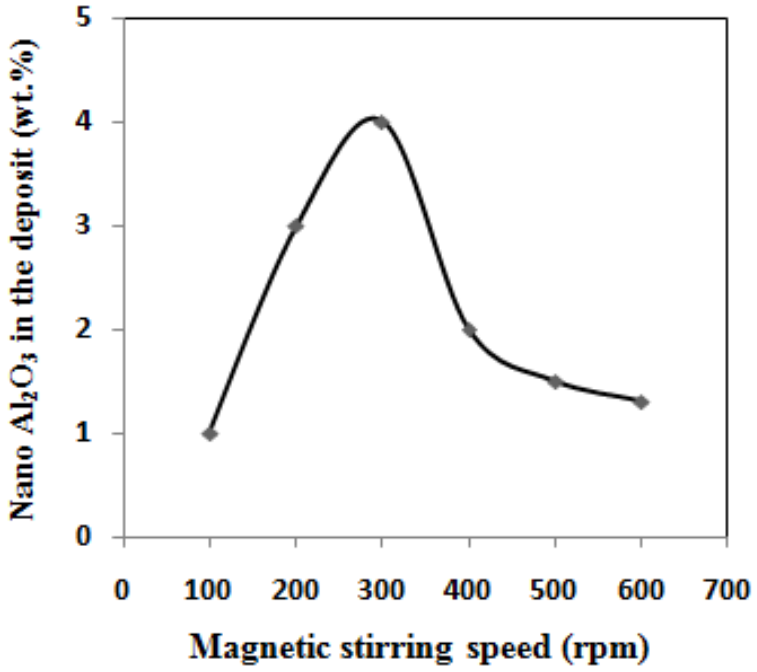

Figure 13. Effect of bath agitation speed on the nano Al_2O_3 content in the deposit.

The experimental results presented in Fig. 13 show that the increase in stirring rate of bath solution enhances particle transport, and causes an increase in the amount of incorporated Al_2O_3 nanoparticles in the coat. However, at too high stirring rates (>300 rpm) nanoparticles will not have enough time to be attracted to the surface in order to be embedded in the coat matrix with a subsequent decrease in the level of particle co-deposition in the coat. Additionally, apart from particles transportation agitation has a supplementary role of maintaining the nanoparticles in a uniformly dispersed suspension throughout the plating bath. Increasing the dispersability of Al_2O_3 nanoparticles would prevent their agglomeration, which is necessary to obtain homogenous deposit with a good distribution of nanoalumina inside its microstructure [35]. On the other hand, very low stirring rate allows settling down of the nanoparticles and also higher probability for their agglomeration.

3.6. Effect of nickel ion concentration

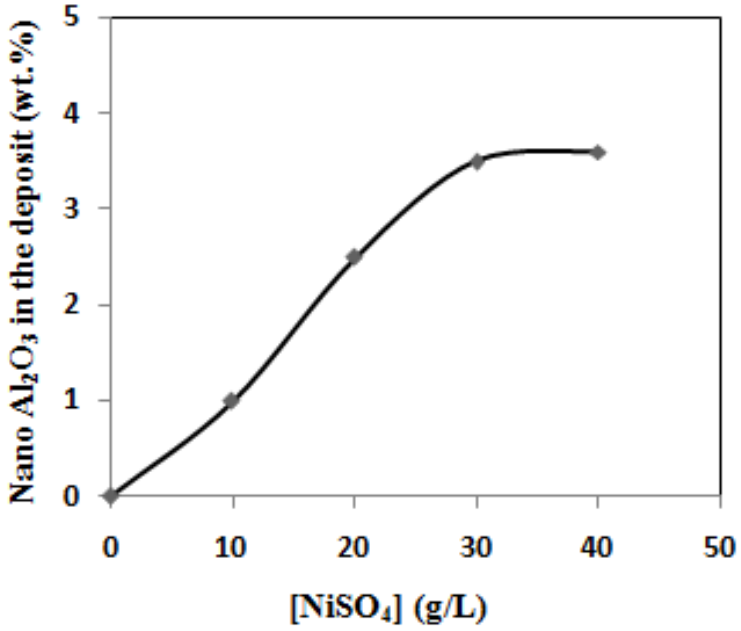

Figure 14. Effect of nickel sulfate concentration in the electroless plating bath on the nano Al_2O_3 content in the deposit.

Experimental results in Fig. 14 illustrate that the amount of Al_2O_3 nanoparticles deposited inside the Ni-P matrix increases with increasing nickel ion concentration in the plating solution. This can be attributed to increase in the amount of adsorbed metal ions on the nanoparticles. Besides, the density (ρ_e) and viscosity (η) of solution in the EN bath are both increased with increasing concentration of dissolved $NiSO_4$ salt, which is the source of nickel ion in the bath. Therefore, based on Stokes law [37] the suspension stability would increase with decreasing settling speed of the particles (γ) as given by the Stokes equation of sedimentation, being expressed as: $\gamma = \frac{2gr_p^2(\rho_p - \rho_e)}{9\eta}$, where g is the acceleration of gravity, r_p and ρ_p are the particle radius and density, respectively. It follows that the suspension stability depends directly on the electrolyte density (ρ_e) and its viscosity (η), so that as these two values are increased the settling speed of the particles becomes slower and suspension stability increases.

3.7. Corrosion performance

Fig. 15 presents the potentiodynamic polarization curves of AZ91D magnesium alloy in 3.5 wt.% NaCl solution for both bare and some selected coated samples. The effect of heat treatment on the polarization behavior of those nanocomposite coatings is also depicted in the same figure.

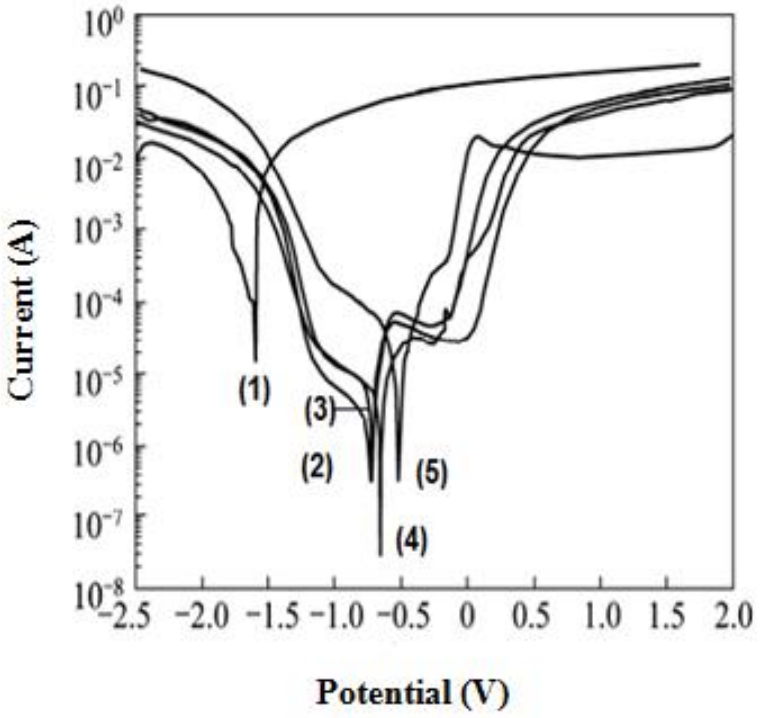

Figure 15. Potentiodynamic polarization curves of AZ91D magnesium alloy in 3.5 wt.% NaCl solution: (1) bare substrate, (2) electroless Ni-P/2 wt.% nano Al_2O_3 composite coated sample as-deposit, (3) electroless Ni-P/2 wt.% nano Al_2O_3 coated sample after heat treatment at 350 ^oC for 1 h, (4) electroless Ni-P/4 wt% nano Al_2O_3 composite coated sample as-deposit, and (5) electroless Ni-P/4 wt.% nano Al_2O_3 composite coated sample after heat treatment at 350 ^oC for 1 h.

Table 1. Corrosion parameters in 3.5 wt.% NaCl solution for non-coated and coated AZ91D substrate with Ni-P/x wt.% nano Al_2O_3 composites as-plated and heat-treated at 350 ^oC for 1h.

Sample	β_c/ mV/dec	β_a/ mV/dec	E_{corr}/ V (vs.SCE)	I_{corr}/ mA	P % [a]
Bare AZ91D substrate	-0.35	0.18	- 1.530	0.392	
2 wt.% nano Al_2O_3 (A)	-0.70	0.15	- 0.572	0.003	99.2
(A) Heat-treated at 350^{o}C	-0.87	0.10	- 0.565	0.005	98.7
4 wt.% nano Al_2O_3 (B)	-0.92	0.27	- 0.531	0.002	99.5
(B) Heat-treated at 350^{o}C	-0.85	0.23	- 0.502	0.004	99.0

[a] P % = 1- $I_{corr(coated)}$ /$I_{corr(bare)}$ x 100 is the degree of protection of the of the coated samples.

Table 1 lists the corrosion parameters, namely the corrosion potential (E_{corr}) and corrosion current strength (I_{corr}) as estimated from the recorded polarization curves of the prepared samples. It is evident from the results of Fig. 15 that each of as-plated and heat treated nanocomposite coated samples show lower anodic passivation potential than its value for the bare AZ91D substrate. On the other hand, each heat treated nanocomposite coated sample (for 1 h at 350 ^oC) exhibits a somewhat

wider passivation potential zone occurring at higher current strength compared with that for the as-plated non-heated similar sample. This indicates that heat treatment has a deleterious effect on the protection capability of the nanocomposite coatings, most likely due to microstructure changes occurred during the heating process. Also from Table 1, it can be observed that either as-plated or heat-treated coated samples show significant positive shift (by ~ 1 V) in E_{corr} towards higher potential value, as well as a sharp decrease in its I_{corr} value compared with values for the uncoated bare AZ91D substrate. The results demonstrate higher degree of surface protection reaching a value between 98.7 – 99.5 % depending on the amount of nano Al_2O_3 in the EN deposit and the post heat-treatment of the coating. Thus, the increase in the content of the co-deposited nanoAl_2O_3 particles in the Ni-P metallic matrix offers more improvment in its corrosion protection performance. For example, for 2 wt.% nanoAl_2O_3 composite the protection efficiency is 99.2 % which increases to 99.5 % for the coating containing 4 wt.% Al_2O_3 nanoparticles. It is evident that nano Al_2O_3 particles embedded in Ni-P alloy can reduce the surface of the corroding part yielding a homogenous structure, and thus afford a potential physical barrier for AZ91D corrosion in the aggressive sodium chloride environment.

In general, post-heat treatment affects negatively the corrosion resistance of any coated sample [38], as it increases slightly its I_{corr} value relative to the unheated as-plated comparable one (Table 1). This indicate that heat treatment process has an adverse effect on the protection efficacy of nanocomposite coatings. Such behavior is likely attributed to the formation of intermetallic Ni_3P phase and possible galvanic attack along the interface of nickel/particles [39], leading to reducing the corrosion stability of the AZ91 alloy substrate.

4. CONCLUSIONS

1- Ni-P/Al_2O_3 nanocomposites on AZ91D magnesium alloy have been synthesized using electroless plating technique with co-deposition of nanoalumina particles. Various plating parameters were studied in order to investigate the impact of these variables on the properties of the prepared coatings.

2. Upon increasing nanoAl_2O_3 concentration in the plating bath its extent in the deposit increases till a maximum value of 4 wt.% at a concentration level of 15 g/L. At higher concentrations possible particle agglomeration in solution occurs leading to decrease the amount of nanoparticles in the deposit. Meanwhile, the composite deposition rate decreases if the load of Al_2O_3 nanoparticles in the plating bath increases over the concentration range 0-20 g/L. Also, the coat micro-hardness and wear resistance are both increase with increasing nano Al_2O_3 concentration in the plating solution.

3. SLS surfactant is used to increase the wettability of nanoparticles, thus preventing their agglomeration and producing a homogenous deposit with a good dispersion of nanoAl_2O_3 inside its microstructure. Addition of SLS at very low concentration of 25 ppm leads also to decrease the porosity of the deposit by almost half its value compared with that for the as-plated sample from nickel bath devoid the surfactant. Further reduction in the porosity of any prepared coat can be achieved after post heat treatment.

4. The corrosion resistance of AZ91D alloy improves significantly after coating with electroless

Ni-P having different nano Al_2O_3 contents. However, after heat treatment the corrosion rate slightly increases for any coated sample compared with the non-heated as-plated similar one, indicating a decrease in the protection performance of the annealed composite coatings caused by the inter-grain galvanic attack.

References

1. P. L. Hagans, C.M. Haas, *Chromate Conversion Coatings*, in.: ASM Handbook, *Surface Engineering*, vol. 5, ASM International (1994) 405.
2. L. M. Abrantes, J. P. Correia, *J. Electrochem. Soc*, 141 (1994) 2356.
3. A. K. Sharma, M. R. Suresh, H. Bhojraj, H. Narayanamurthy, R. P. Sahu, *Met. Finish*., 96 (1998) 10.
4. J. N. Balaraju, T. S. N., Sankara Narayanan, S. K. Seshadri, *J. Appl. Electrochem*., 33 (2003) 807.
5. J. L. Gray, B. Luan, *J. alloys compd*., 336 (2002) 88.
6. L. L. Shreir, R. A. Jarman, G. T. Burstein, *Magnesium and Magnesium Alloys*, in *Corrosion*, Vol. I, Buttermorth-Heinemann Ltd, Oxford, UK (1994) 4:98.
7. E.Ghali, *Magnesium and magnesium alloys*, Ch. 44, in: R.W. Revie (Ed.), *Uhlig Corrosion Handbook*, John Wiley, New York, USA (2000) 793.
8. K. V. Kainer, P. Bala Srinivasan, C. Blawert, W. Dietzel (Eds.), *Corrosion of Magnesium and its Alloys*, in: *Shereir's Corrosion*, Fourth edition, vol. 3, Academic Press, New York (2010) 2011.
9. R. Lindström, L. -G. Johansson, G. E. Thompson, P. Skeldon, J. -E. Svensson, *Corros. Sci*., 46 (2004) 1141.
10. J. Chen, J. Wang, E. Han, W. Ke, *Corrosion*, 63 (2007) 661.
11. L. J. Zhang, J. J. Fan, Z. Zhang, F. H. Cao, J. Q. Zhang, C. N. Cao, *Electrochim. Acta*, 52 (2007) 5325.
12. H. Ardelean, I. Frateur, S. Zanna, A. Atrens, P. Marcus, *Corros. Sci*., 51 (2009) 3030.
13. X. Chen, G. Li, J. Lian, Q. Jiang, *Appl. Surf. Sci*., 255 (2008) 2322.
14. Y. L. Lee, Y. R. Chu, W. C. Li, C. S. Lin, *Corros. Sci.*, 70 (2013) 74.
15. V. Barranco, N. Carmona, J. C. Galván, M. Grobelny, L. Kwiatkowski, M. A. Villegas**,** *Prog. Org. Coat.*, 68 (2010) 347.
16. R. Ambat , W. Zhou, *Surf. Coat. Technol*., 179 (2004) 124.
17. Z. Shao, Z. Cai, R. Hu, S. Wei, *Surf. Coat. Technol*., 249 (2014) 42.
18. W.-J. Cheong, B. L. Luan, D.W. Shoesmith, *Corros. Sci*., 49 (2007) 1777.
19. D. Seifzadeh, Z. Rajabalizadeh, *Surf. coat. Technol*., 218 (2013) 119.
20. Z.-H. Xie, F.Chen, S.-R. Xiang, J.-L. Zhou, Z.-W. Song, G. Yub, *J. Electrochem. Soc*., 162 (2015) D115.
21. C. T. J. Low, R. G. A. Wills, F. C. Walsh, *Surf. Coat. Technol*., 201 (2006) 371.
22. F. Erler, C. Jacob, H. Romanus, L. Spiess, B. Wielage, T. Lampke, S. Steinhauser, *Electrochim. Acta*, 48 (2003) 3063.
23. J. N. Balaraju, Kalavati, K. S. Rajam, *Surf. Coat. Technol*., 200 (2006) 3933.
24. Y. de Hazan, D. Zimmermann, M. z'graggen, S. Ross, C. Aneziris, H. Bollier, et al., *Surf. Coat. Technol*., 204 (2010) 3464.
25. N. El Mahallawy, A. Bakkar, M. Shoeib, H. Palkowski, V. Neubert, *Surf. Coat. Technol*., 202 (2008) 5151.
26. Z. Abdel Hamid, , *J. Metall. Eng*. (ME), 3 (2014) 29.
27. S. Afroukhteh, C. Dehghanian, M. Emamy, *Progress in Natural Science: Mater. Inter*., 22 (2012) 318.
28. Y. C. Wu, G. H. Li, L. Zhang, B. Yan, *Mater. Res. Adv. Tech*., 91 (2000) 788.

29. J. P. Celis, J. R. Roos, *J. Electrochem. Soc.,* 124 (1977) 1508.
30. J. P. Celis, J. R. Roos, C. Buelens, *J. Electrochem. Soc.*, 134 (1987) 1402.
31. J. Li, Y. Tian, Z. Huang, X. Zhang, *Appl. Surf. Sci.***,** 252 (2006) 2839.
32. P. Gadhari, P. Sahoo, *Inter. J. Mater. Chem. Phy.*, 1 (2015) 1.
33. Z. Liu, W. Gao, *Surf. Coat Technol*., 200 (2006) 5087.
34. I. Apachitei, J. Duszczyk, L. Katgerman, P. J .B. Overkamp, *Scripta Materialia*, 38 (1998) 1347.
35. T. Radu, M. Vlad, F. Potecasu, G. G. Istrate, *Digest J. Nanomater. Biostr*., 10 (2015) 1055.
36. S. K. Das, N. Putra, P. Thiesen, W. Roetzel, *J. Heat Transfer*, 125 (2003) 567.
37. H. Lamb, *Hydrodynamics* (6th ed.), Cambridge University Press (1994).
38. A. S. Hamdy, M. A. Shoeib, H. Hady, O. F. Abdel Salam, *Surf. Coat. Technol.,* 202 (2007) 162.
39. F. Erler. C. Jakob, H. Romanus, L. Spiess, B. Wielage, T. Lampke, S. Steinhauser**,** *Electrochim. Acta*, 48 (2003) 3063.